

PAPER • OPEN ACCESS

Simplified algorithm for determining injection duration to achieve fast response in SI engines

To cite this article: Omar Shawky 2020 *IOP Conf. Ser.: Mater. Sci. Eng.* **973** 012005

View the [article online](#) for updates and enhancements.

You may also like

- [Three-layer Authentication in Keystroke Dynamics using Time based Tool](#)
Namisha Bhasin and Sandhya Tarar
- [Design of Automatic Plant Areas Using Humidity Sensor Based On Internet of Thing](#)
G Gunawan, Marliana Sari, Benar Surbakti et al.
- [Ultrasound device selection by using F-ANP and COPRAS](#)
Humala L Napitupulu



The banner features a dark blue background on the left with white and orange text, and a photograph of a woman at a podium on the right. The woman is smiling and looking towards the camera. The podium has a laptop on it. The background of the photo is a bright, modern interior.

ECS The Electrochemical Society
Advancing solid state & electrochemical science & technology

243rd Meeting with SOFC-XVIII

Boston, MA • May 28 – June 2, 2023

Accelerate scientific discovery!

Learn More & Register

Simplified algorithm for determining injection duration to achieve fast response in SI engines

Omar Shawky

DLECS - Cairo university

engomar582@gmail.com

Abstract. For modern SI engines, the injection duration and its timing are one of the most important parameters which influence the mixture homogeneity, emissions, combustion efficiency, and engine response. In the present work, a simplified port fuel injection system with its driver algorithms was designed to control the injection duration and its timing. The Calibrated Dose method is used in this system instead of the stream mixing method. Therefore, the injected fuel mass is accurately computed according to the engine load, engine speed, engine operating condition, and the amount of air drawn into the engine. The system consists of a conventional port fuel injection system equipped with a micro-controller, a Throttle Position Sensor (TPS), a couple of Hall Effect Sensors (HES), load cell with its driver module, injector controller circuit, and a custom-made inlet port. The micro-controller is used to calculate the injection duration each engine cycle according to engine speed, amount of air drawn per cycle and engine load. The two HES are used to detect the injection timing and measure the engine speed. The TPS is used to monitor the throttle position angle so it can calculate the amount of air drawn into the engine at that time with respect to engine speed. The load cell and its driver module are used to measure the engine torque and consequently the brake power. The injector controller circuit is used to initiate the injection process at the perfect timing for the accurate duration.

1. Introduction

For the sake of improving energy conversion efficiency in the transportation sector, many fuel systems were developed to increase combustion efficiency and engine response [1]. The transportation sector is strongly dependant on fossil fuels especially gasoline and diesel [2]. The passenger transportation sector tends to spark-ignition (SI) engines [3] which runs on gasoline. Therefore, engine developers always target to minimize fuel consumption and lower engine emissions [4]. For the SI engines specifically, one of the most effective parameters to decrease the fuel consumption is the accurate fuel injection duration [5] and its timing [6]. Also, the air to fuel ratio suitable to the engine operating conditions is so important to decrease fuel consumption [7]. SI engines use mainly two fuel injection strategies; the port fuel injection (PFI) strategy, and the gasoline direct injection (GDI) strategy [8-11]. The PFI systems are easier to manufacture and design than the GDI systems [12]. PFI technology is widely spread in the SI engines to reduce fuel consumption and increase the output power [13].

In this system, the engine is equipped with an electronic control unit consisting of a micro-controller, monitoring sensors and actuators [14]. The micro-controller, called as the engine control unit (ECU) [15], continuously detects what the driver is demanding out of the engine [16]. Accordingly, it processes the data received from the engine inputs such as airflow rate, fuel flow rate, throttle position and engine temperature [17]. The micro-controller uses this processed data to trigger the injection process at the accurate timing and for the suitable duration whereas the precise injection



timing greatly influences the engine performance [18]. The time available for injection and mixing is very short also the size of droplets affects the combustion efficiency [19], therefore the faster the injection response, the better the combustion efficiency [20] which results in more power output [21]. The engine cold start condition also affects fuel consumption as the fuel atomization is reduced due to the engine's low engine temperature [22].

There were many attempts made to enhance the PFI for the small motorcycles to increase the compatibility, efficiency and decrease fuel consumption [23]. In the present work, a simplified port fuel injection system was designed and coded to achieve a fast-responsive injection process with variable load and speed.

2. Description of the proposed system

The proposed system aims to inject just the suitable amount of fuel at the accurate timing. The suitable fuel mass depends on many factors: air mass drawn, engine speed, required power, and air to fuel ratio. The control methodology is the Calibrated Doze method. This method handles each of these factors carefully to calculate the suitable fuel mass.

The present work was conducted on a carbureted internal combustion engine. The carburetor was replaced by the proposed port injection system. The engine used was a four-stroke SIE. The engine specifications are shown in table 1.

Table 1. Engine Specifications.

Model	GX390
Type	4-stroke, overhead valve, single-cylinder, horizontal shaft
Cooling system	Air cooling
Bore& Stroke	82·64 mm
Rated power	8.2/3600 (KW/rpm)
Maximum torque	27.1/2500 (N.m/rpm)
Displacement	389 cc
Compression ratio	8.0:1
Ignition system	Spark
Oil capacity	1.1L
Lubrication system	Splash
Starting	Kicking starting
Dimensions	405·450·443
Dry weight	31 kg

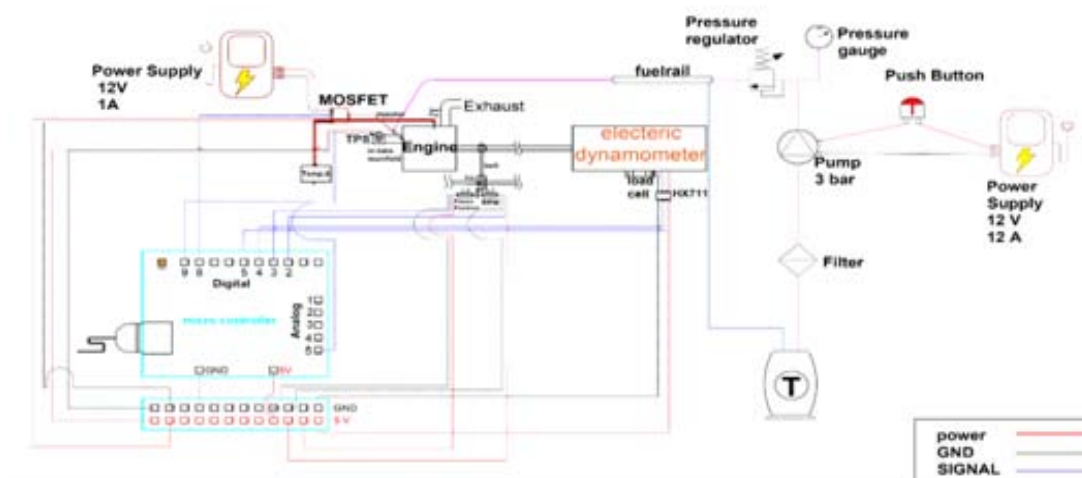


Figure 1. Detailed view for the proposed PFI system.

The proposed injection system consists of a conventional port injection system equipped with simplified control system. The control system is implemented using integrated electrical components for measuring engine inputs and outputs as shown in figure 1.

3. The proposed system methodology

The control system methodology is the Calibrated Doze method. This method consists of three steps to determine the suitable fuel mass. It begins with calculating the air mass, then it determines the air to fuel ratio suitable for engine operating conditions, at the end it determines the adequate fuel mass. The below points show how the method is implemented in the code. Each one of these points is explained in the coming subsections.

- Calculating the amount of air drawn per cycle per cylinder.
- Determining the air to fuel ratio according to the load and engine speed.
- Determining the accurate fuel mass suitable to the drawn air mass and the determined air to fuel ratio and then calculating the accurate injection duration to inject the determined fuel mass.
- Feedback and monitoring the outgoing parameters during engine operation. (mass of air - air to fuel ratio- calculated fuel mass - injection duration - engine speed in rpm - measured engine torque - brake power - engine temperature – engine throttle position).

3.1. Calculating air mass drawn into the engine cylinder

To calculate the amount of air drawn into the engine cylinder, the volumetric efficiency must be determined. There are two main factors greatly affecting the volumetric efficiency: the engine throttle position angle and the engine speed. The engine throttle position is determined using the TPS and the engine speed is computed using a HES. A function between the volumetric efficiency, engine throttle position, and engine speed was formulated by measuring the actual amount of air drawn into the cylinder by using an external anemometer then comparing these results to the output of the following equation:

$$\dot{m}_{\text{calc}} = \rho_{\text{air}} \cdot V_{\text{st}} \cdot \eta_v \quad (1)$$

Where \dot{m}_{calc} the calculated amount of air, ρ_{air} the ambient air density, V_{st} the engine stroke volume and η_v the volumetric efficiency. By this comparison, the volumetric efficiency for all the engine speed range and different throttle position angles was formulated as shown in figure 2.

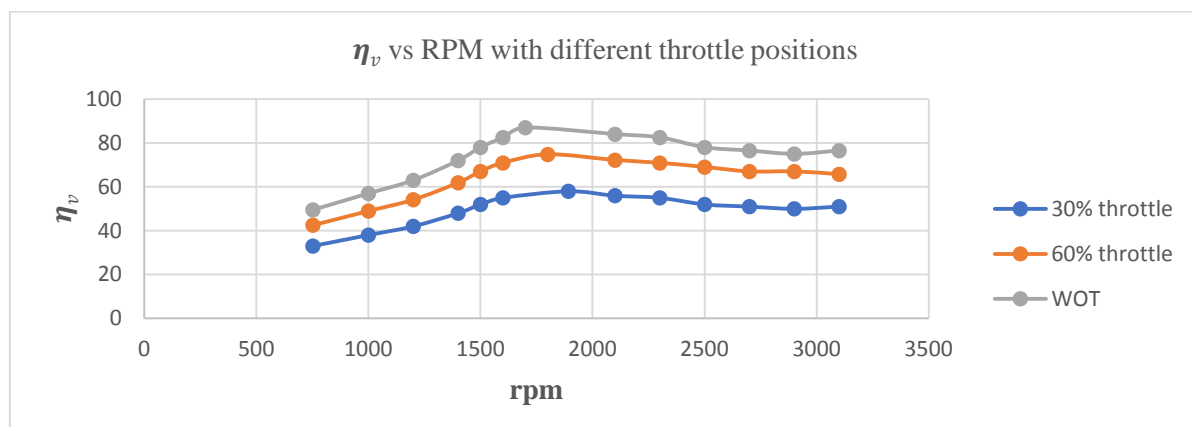


Figure 2. Curve fitting for volumetric efficiency vs RPM at different throttle position angles.

After this experimental calibration, three functions were developed at 30%, 60%, and WOT (Wide Open Throttle) as follow.

- At 30% throttle position angle:

$$\eta_v = (-18 \cdot 10^{-3} \cdot RPM^6) + (-14 \cdot 10^3 \cdot RPM^5) - (RPM^4 \cdot 10^{-2}) + (-7 \cdot 10^3 \cdot RPM^3) + (3 \cdot 10^{-3} \cdot RPM^2) + (0.1385 \cdot RPM) - 8.5545 \quad (2)$$

- At 60% throttle position angle:

$$\eta_v = (-18 \cdot 10^{-3} \cdot RPM^6) + (-14 \cdot 10^3 \cdot RPM^5) - (RPM^4 \cdot 10^{-2}) + (-7 \cdot 10^3 \cdot RPM^3) + (3 \cdot 10^{-3} \cdot RPM^2) + (0.1935 \cdot RPM) - 13.709 \quad (3)$$

- At WOT:

$$\eta_v = (-18 \cdot 10^{-3} \cdot RPM^6) + (-14 \cdot 10^3 \cdot RPM^5) - (RPM^4 \cdot 10^{-2}) + (-7 \cdot 10^3 \cdot RPM^3) + (3 \cdot 10^{-3} \cdot RPM^2) + (0.204 \cdot RPM) - 12.346 \quad (4)$$

In equations (2), (3) and equation (4), there are four constant parameters and the last two parameters are changing with respect to the engine throttle position angle. So, a generic equation was formulated between the volumetric efficiency, engine speed, and engine throttle position angle. The generic function will be like equation (5).

$$\eta_v = (-18 \cdot 10^{-3} \cdot RPM^6) + (-14 \cdot 10^3 \cdot RPM^5) - (RPM^4 \cdot 10^{-2}) + (-7 \cdot 10^3 \cdot RPM^3) + (3 \cdot 10^{-3} \cdot RPM^2) + ((A) \cdot RPM) - (B) \quad (5)$$

where, A and B are functions of throttle position angle. Equation (6) and (7) were formulated to relate variable A and variable B with the throttle position angle.

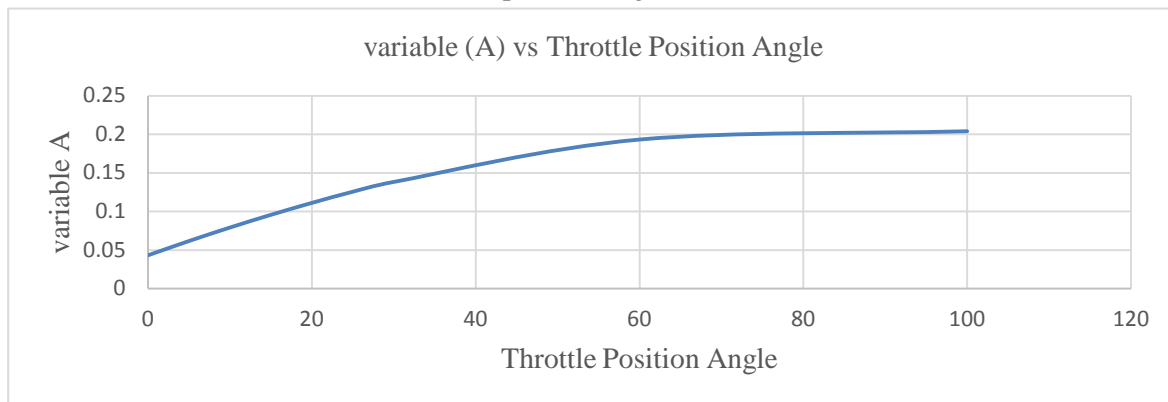


Figure 3. Curve fitting for the relation between variable A and TPS.

After the curve fitting for the experimental data, equation (6) was generated:

$$A = (-0.0029 \cdot (TPS^2)) + (0.4365 \cdot TPS) - 1.894 \quad (6)$$

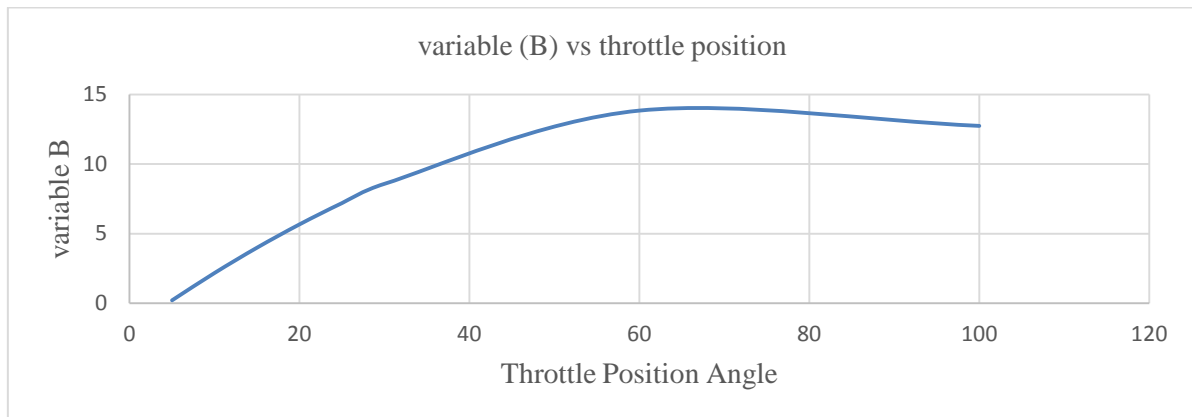


Figure 4. curve fitting for the relation between variable B and TPS.

After the curve fitting for the experimental data, equation (7) was generated:

$$B = \left((-2 \cdot 10^{-5}) \cdot (\text{TPS}^2) \right) + (0.0038 \cdot \text{TPS}) + (0.0433) \quad (7)$$

Using equation (5), (6), and (7), the air mass drawn is calculated accurately.

3.2. Determination of the air to fuel ratio

In order to relate the mass of air drawn to the fuel mass required, the accurate air to fuel ratio is required. This air to fuel ratio was obtained by measuring the amount of air drawn into the engine by an external anemometer and the amount of fuel consumed at a specific time and a specific throttle position with constant engine speed at 3000 RPM, Then these actual data were used to generate a function between the air to fuel ratio and the throttle position as shown in figure 5.

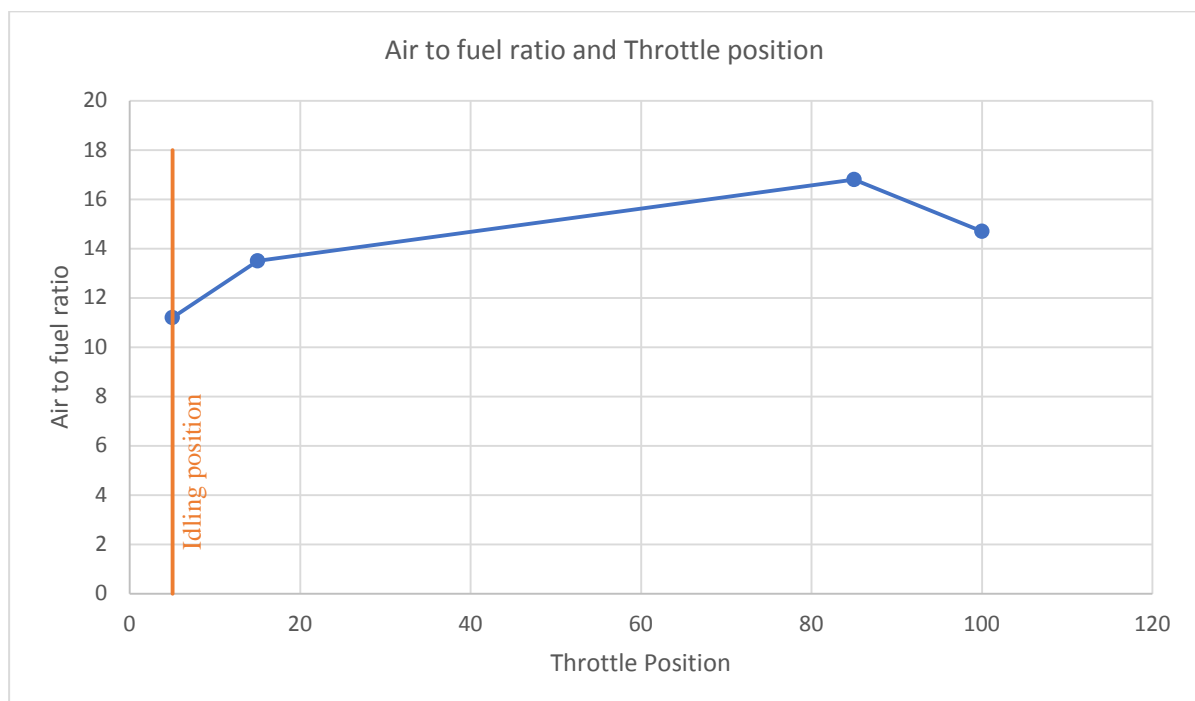


Figure 5.The air to fuel ratio at each throttle position with constant engine speed.

As shown in figure 5 the suitable air to fuel ratio was determined at each engine throttle position, and the ideal air to fuel ratio is 14.7.

3.3. Determination of the accurate fuel mass and injection duration

The accurate fuel mass is calculated using equation (8).

$$\text{fuel mass} = \frac{\text{calculated air mass}}{\text{assigned air to fuel ratio}} \quad (8)$$

After the fuel mass calculation, the injection duration is to be determined. This is achieved by using a dedicated circuit developed for this process. This circuit is used to control the injection timing and duration as shown in figure 6. An injector calibration must be done to determine the injection duration suitable for each fuel mass calculated. The used injector has 4 holes each one has a diameter of 0.1mm. As shown in figure 7 and table 2, the function between the injection duration and the fuel mass is nearly linear.

Table 2. Experimental calibration data showing the injection duration for each fuel mass.

fuel mass in grams per injection process (1/2000)	fuel mass in grams for the hole 2000 injection process	time (milliseconds) injection duration
0.002	4	2
0.0035	7	3
0.005	10	4
0.007	14	5
0.0085	17	6
0.0105	21	7
0.0125	25	8
0.014	29	9
0.016	32	10
0.0175	35	11
0.019	38	12

Calibration process:

- A code was developed to inject 2000 times.
- The injection duration was changed from 2 milliseconds to 10 milliseconds each injection cycle with constant injection time off as 10 milliseconds.
- The injected amount of fuel was weighed then divided by 2000 to get the weight of each injection process as shown in table 2.
- As shown in figure 7, formulating a function between the injection duration and the injected fuel mass according to the experimental results.

After this calibration, a function between the injection duration and fuel mass was generated as shown in equation (9).

$$\Delta t_{Inj} = 572.28 \cdot m_{fuel} + 0.9911 \quad (9)$$

Where, Δt_{Inj} is the injection duration in milliseconds and m_{fuel} mass of fuel in grams. Equation (9) will determine the suitable injection duration for each fuel mass required.

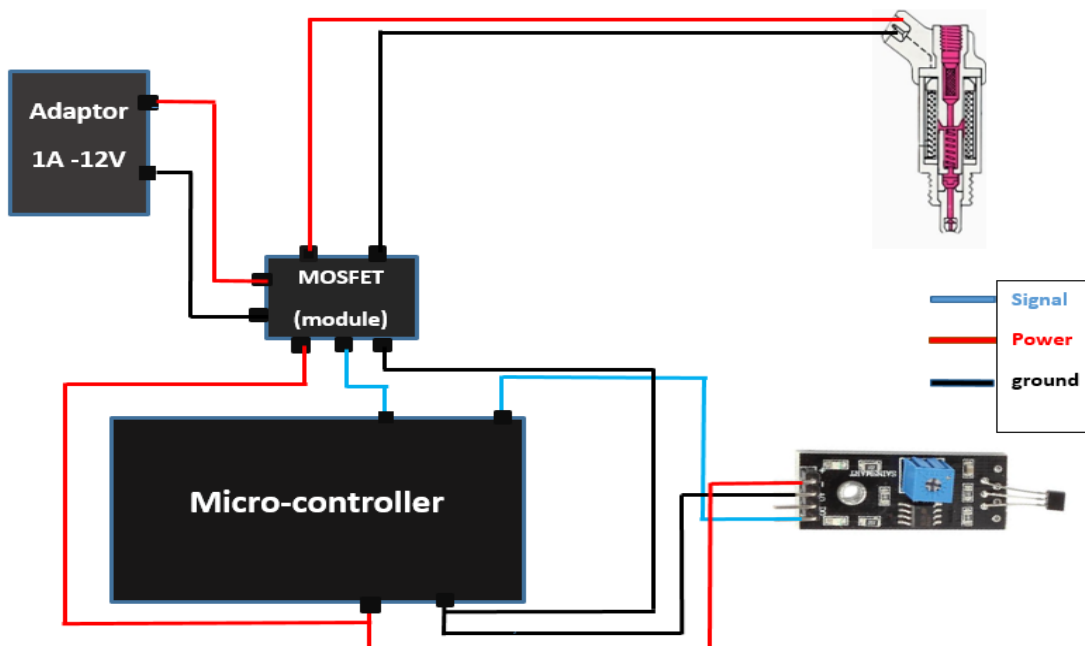


Figure 6. simplified injection circuit.

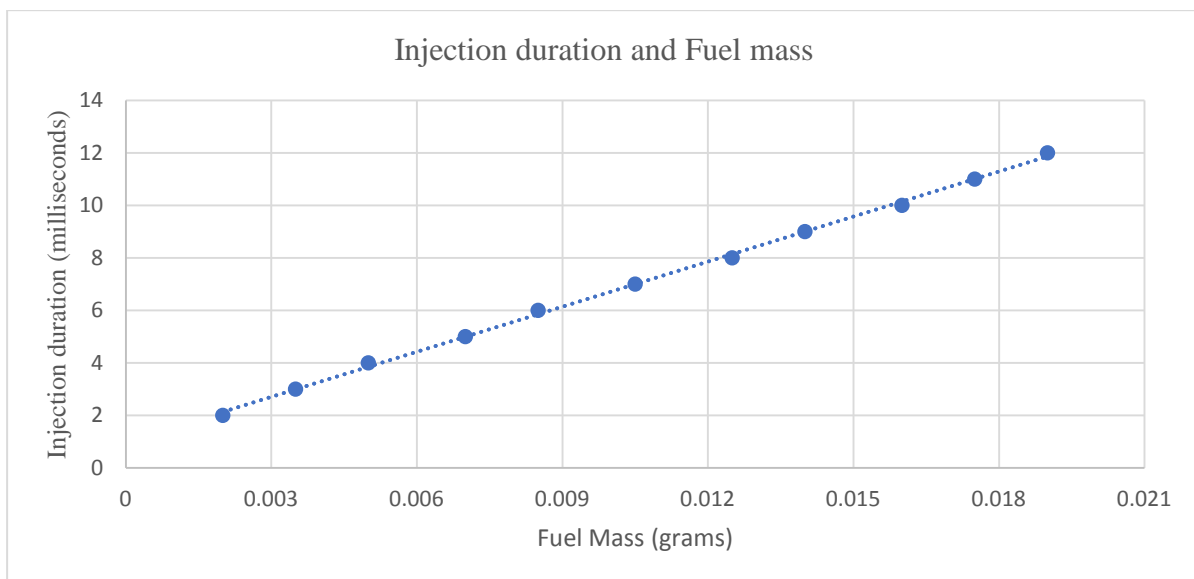


Figure 7. Curve fitting to formulate a function relating the amount of fuel and the injection duration.

After the injection duration is calculated, the injection timing is required. A HES is used to detect the beginning of the intake stroke from the red sign, magnet, on the external gear. The beginning of intake stroke is the beginning of the injection process. To represent all the cycle events within a single revolution, an external gear is used as shown in figure 8. During the engine operation, the HES detects the suction stroke beginning each cycle. Then it sends a signal to the micro-controller and consequently to the injector driver circuit which will initiate the injection process for the determined injection duration. The injection process is initiated by opening the injector solenoid using the external voltage supply as shown in figure 6.

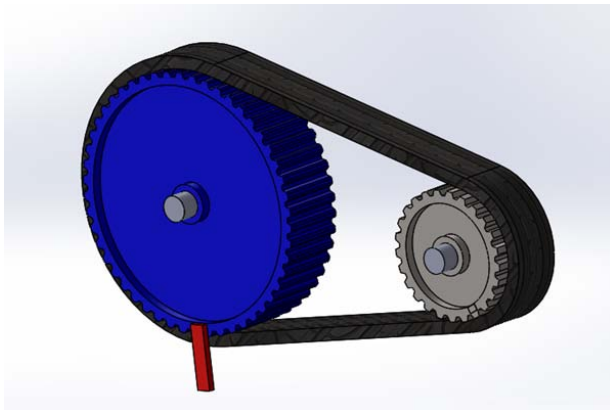


Figure 8. The reduction ratio between the external gear and the crankshaft gear, and the place of the magnet red sign.

3.4. Measuring the basic engine parameters

3.4.1. *Load measurement.* A load cell was used to measure the engine torque. A torque arm was used to transfer the engine torque to the load cell. One end of it was mounted on an electrical dynamo-meter body and the other was mounted on the load cell. Using this arrangement and the equation (10),

$$\mathbf{T = F \cdot L} \quad (10)$$

Where, T is the engine torque and F is the force acting on the iron arm by the electrical dynamo-meter body and L The iron arm length.

3.4.2. *Engine speed measurement.* Another HES was used to detect the end of each cycle and record its time in microseconds by using another sign 'magnet'. By comparing the end time of each cycle and the previous cycle, the periodic time is calculated. Substituting in the frequency formula as shown in equation (11).

$$\mathbf{F = \frac{1}{T}} \quad (11)$$

where F The frequency and T The periodic time. The engine frequency is obtained, so consequently the engine speed in revolution per minute is calculated by using equation (12).

$$\mathbf{RPM = F \cdot 60 \cdot 2} \quad (12)$$

The result was multiplied by 2 due to the reduction ratio done by external gear.

3.4.3. *Monitoring engine temperature.* The engine temperature was monitored by using a spark-plug temperature sensor, installed between the spark-plug and the upper surface of the engine cylinder head as shown in figure 9.a. The sensor itself is shown in figure 9.b



Figure 9.a. Spark plug temperature sensor installation.



Figure 9.b. The spark plug sensor.

The temperature sensor is updated each millisecond. The temperature also controls the engine status. When the engine temperature is low, the air to fuel ratio is changed to be slightly rich until the engine reaches the ideal operating temperature. After reaching this condition, the engine status will be changed to warm status so the air to fuel ratio will be leaner than the cold status to achieve the least possible fuel consumption.

All the previous parameters are outputs of the used sensors except for the brake power so it will be calculated using equation (13).

$$P = T \cdot \omega \quad (13)$$

where P the brake power, T the engine torque, obtained by the load cell, and ω the angular velocity.

The angular velocity is obtained using equation (14).

$$\omega = \left(\frac{2 \cdot \pi \cdot N}{60} \right) \quad (14)$$

where N is the engine speed in rpm, obtained by the HES.

3.5. Monitoring the outgoing parameters during engine operation

Now, it is easy to monitor the engine parameters every specified period. The mass of air drawn per cycle is calculated in grams. The air to fuel ratio is determined to be suitable for the current engine load and engine throttle position using the equation (8). The accurate fuel mass in grams is calculated with respect to the determined air to fuel ratio. The injection duration is determined using equation (9). Engine speed in rpm was measured using a HES. The engine output torque is measured through the load cell. Brake power was determined by engine torque and speed. Engine temperature was measured by a spark plug temperature sensor. These parameters were used to measure system efficiency compared with other systems.

4. Code flow chart

As shown in figure 10, a simple flow chart describes the developed code. First, the code reads the current engine speed, engine temperature, and throttle position angle. Then, it compares the engine temperature to the ideal engine temperature. After this comparison, the code decides the engine operating condition if it is a warm status or a cold start one. for the warm condition, the code calculates the accurate amount of air drawn into the engine then determines the air to fuel ratio according to the engine load, then it calculates the suitable fuel mass required and the suitable injection duration for it. At last, the code waits for the signal from the HES to start the injection process. After each injection process, the engine output torque is measured. For the cold start condition, the code opens the fuel injector for longer durations to make a rich mixture. This rich mixture is used to warm up the engine to the desired engine temperature. Every 30 seconds, all the engine parameters 'calculated or measured' are monitored.

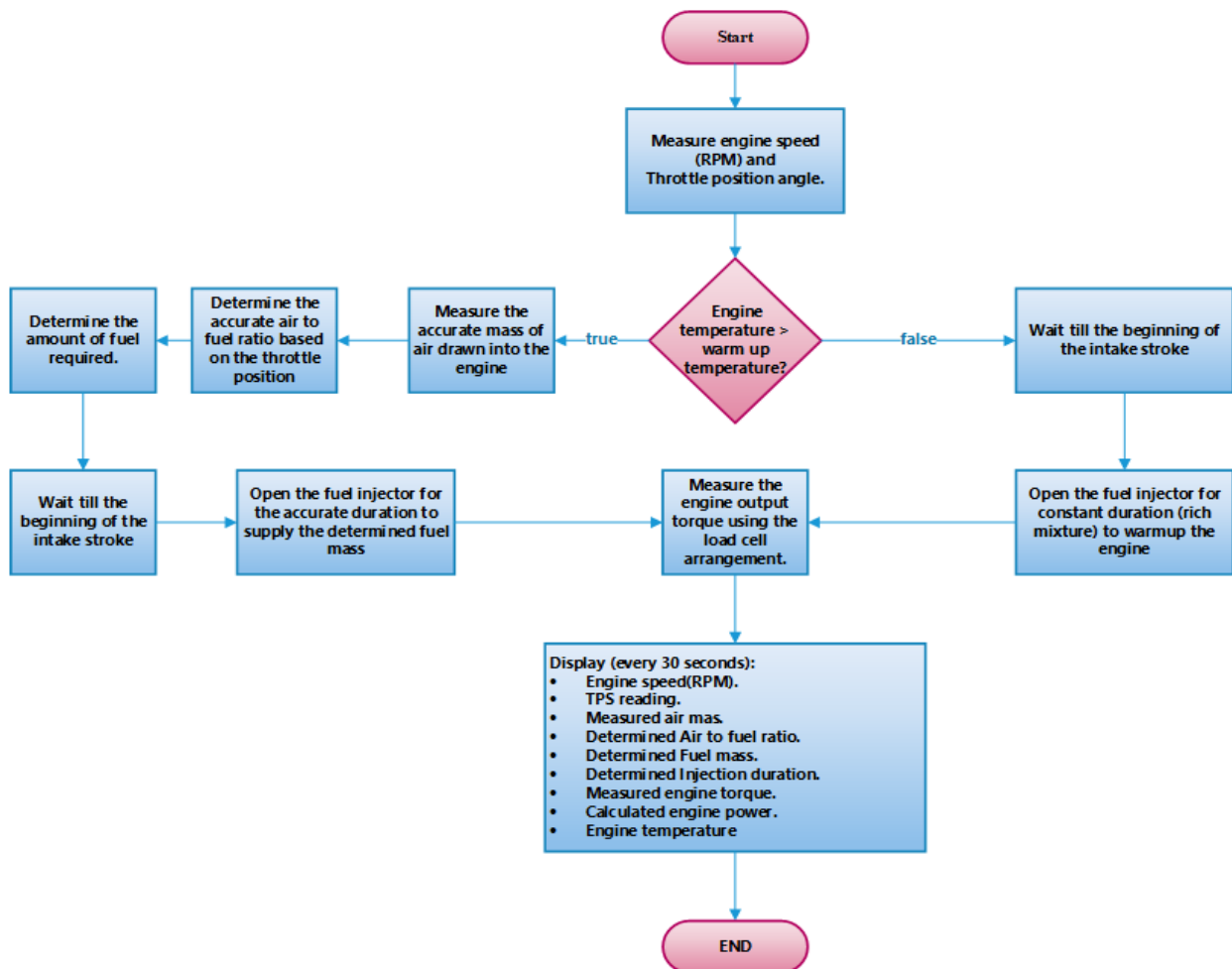


Figure 10. Flow chart for the code.

5. Results

As shown in figure 11, while using the PFI technique, the maximum brake torque is increased by 8%. It is also noticed that the torque in the conventional carburetor system reaches its maximum value at 3000 rpm while the proposed PFI system reaches its maximum torque at 2800 rpm which is more practical in different applications. The maximum brake torque is reached at 2800 rpm while using the PFI system because this system is based on the Calibrated Dose method which will inject just the accurate amount of fuel suitable for the drawn air. Also, the high-pressure injection just above the inlet valve results in a fast response to load compared to the system based on the stream mixing methods.

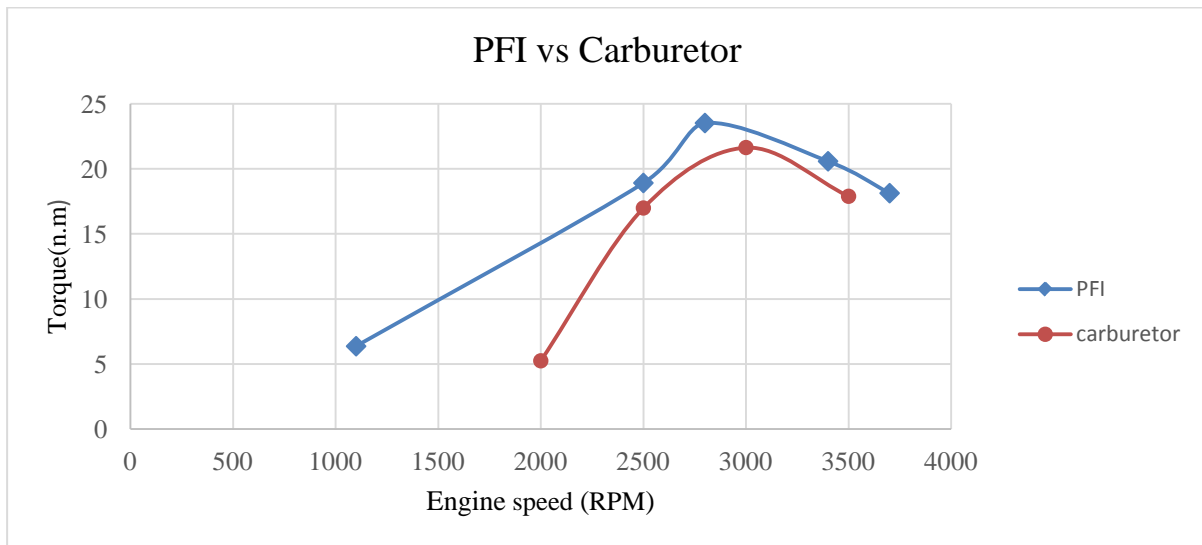


Figure 11. Comparison between the output brake torque by using the proposed PFI system and the carburetor with respect to engine speed at (WOT).

As shown in figure 12, while using the PFI technique, the maximum brake power is increased by 7%. It is also noticed that the maximum brake power in the conventional carburetor system reaches its maximum value at 3000 rpm while the proposed PFI system reaches its maximum torque at 3500 rpm which gives the proposed PFI system a wider engine speed range to control. The PFI system achieves more brake power as it delivers the accurate fuel mass 'suitable for the drawn air just' above the inlet valve. This results in a more homogeneous mixture of fuel and air without losses due to friction of the inlet port walls. Also, the high-pressure injection helps to achieve the fuel atomization to increase mixture quality.

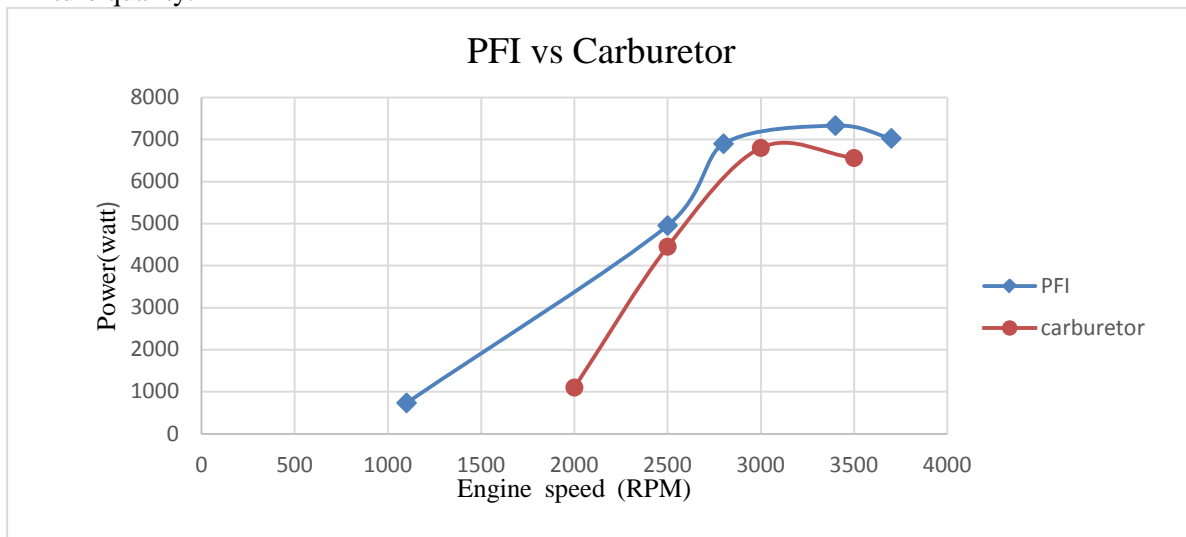


Figure 12. Comparison between the output brake power by using the proposed PFI system and the carburetor with respect to engine speed at (WOT).

6. Conclusion

The proposed algorithm for operating the PFI system has proven to be effective in increasing the specific power over wide range of speed. The proposed PFI system also results in higher brake torque for a wider engine speed range. Using the PFI technique, faster engine response is achieved compared to the carburetor system. Due to using the Calibrated Dose method instead of the stream mixing

method, the used algorithm for operating the PFI system results in lower fuel consumption. The designed algorithm for operating the PFI system could be used for increasing the output torque and power for the same engine block.

7. References

- [1] Zhu R Hu J Bao X He L Lai Y Zu L and Su S 2016 Tailpipe emissions from gasoline direct injection (GDI) and port fuel injection (PFI) vehicles at both low and high ambient temperatures *Environmental Pollution* **216** pp 223–234
- [2] Gupta T Kothari A Srivastava D K and Agarwal A K 2010 Measurement of number and size distribution of particles emitted from a mid-sized transportation multipoint port fuel injection gasoline engine *Fuel* **89** (9) pp 2230–2233
- [3] Nakao Y, Sakurai Y, Hisano A, Saitou M, Kazari M, Murase T and Suzuki K 2016 Effects of Port Injection Specifications on Emission Behavior of THC *SAE International Journal of Engines* **9**(4) p 2427–2433
- [4] Guzzella L and Onder C H 2004 *Introduction to Modeling and Control of Internal Combustion Engine Systems* (Springer-Verlag Berlin Heidelberg) pp 173–221
- [5] Movahednejad E Ommi F Hosseinalipour M and Samimi O 2006 Experimental and Theoretical Study of Injection Timing on Performance and Exhaust Emissions in a Port-Injected Gasoline Engine *ASME 2006 Internal Combustion Engine Division Spring Technical Conference (ICES2006)*
- [6] Cowart J S and Hamilton L J 2006 Post Fuel Injection Fuel Vaporization Characteristics in the Intake Port of a Port-Fuel-Injected *Gasoline CFR Engine ASME Internal Combustion Engine Division Fall Technical Conference (ICEF2006)*
- [7] Feng D, Wei H, Pan M, Zhou L and Hua J 2018 Combustion performance of dual-injection using n-butanol direct-injection and gasoline port fuel-injection in an SI engine *Energy* **160** pp 573-581
- [8] *US6959693B2 Fuel injection system and method.* <https://patents.google.com/patent/US6959693B2/en>
- [9] Mathivanan K Mallikarjuna J M & Ramesh A 2016 Influence of multiple fuel injection strategies on performance and combustion characteristics of a diesel fuelled HCCI engine *Experimental Thermal and Fluid Science* **77** pp 337-346
- [10] Fanick R, Kroll S, Swarts A, and Quarderer S 2019 Effects of Dual Port Injection and Direct-Injection Technology on Combustion Emissions from Light-Duty Gasoline Vehicles *SAE Technical Paper 2019-01-0999*
- [11] Zabeu C, Camargos L, Marinsek L, Berti R et al. 2017 Influence of Injection Timing on the Engine Efficiency and Emissions in a SI PFI Engine Using Ethanol-Gasoline Blends with Several Water Content Levels *SAE Technical Paper 2017-36-0147*
- [12] Kim N ,Cho S ,Choi H, Song H H and Min K 2014 The Efficiency and Emission Characteristics of Dual Fuel Combustion Using Gasoline Direct Injection and Ethanol Port Injection in an SI Engine *SAE Technical Paper 2014-01-1208*
- [13] *US6691021B2 Failure determination system, failure determination method and engine control unit for variable-cylinder internal combustion engine.* <https://patents.google.com/patent/US6691021B2/en>
- [14] *US6763707B2 Failure determination system and method for internal combustion engine and engine control unit.* <https://patents.google.com/patent/US6763707B2/en>
- [15] Anand T and Ravikrishna R 2012 Modelling of mixture preparation in a small engine with port fuel injection *Progress in Computational Fluid Dynamics, An International Journal (PCFD)* **12** No. 6 pp375-388
- [16] Balluchi A, Benvenuti L, Benedetto M D, Pinello C and Sangiovanni-Vincentelli A 2000 Automotive engine control and hybrid systems: challenges and opportunities *Proceedings of the IEEE* **88** Issue 7 pp 888-912 doi: 10.1109/5.871300.

- [17] Movahednejad E, Ommi F, Hossinalipour M and Karbasforoushha M 2005 Experimental and Theoretical Study of Injection Parameters on Performance and Fuel Consumption in a Port-Injected Gasoline Engine *SAE Technical Paper* **2005-01-3805**
- [18] Daniel R Wang C Xu H & Tian G 2012 Effects of Combustion Phasing, Injection Timing, Relative Air-Fuel Ratio and Variable Valve Timing on SI Engine Performance and Emissions using 2,5-Dimethylfuran *SAE International Journal of Fuels and Lubricants* **5** Issue 2 pp 855-866.
- [19] Huang Y Hong G and Huang R 2015 Numerical investigation to the dual-fuel spray combustion process in an ethanol direct injection plus gasoline port injection (EDI+GPI) engine *Energy Conversion and Management* **92** pp 275-286
- [20] Patel R J and Brahmhatt P 2019 Effect of Varying Fuel Injection Timing on Engine Performance of CNG Direct Injection in Retrofitted SI Engine *European Journal of Sustainable Development Research* **3** Issue 3 Article No: em0089
- [21] Dernette J, Mounaim-Rousselle C, Halter F and Seers P 2009 Evaluation of Butanol–Gasoline Blends in a Port Fuel-injection, Spark-Ignition Engine *Oil & Gas Science and Technology* **65**(65) pp 345-351
- [22] Gupta T Kothari A Srivastava D K & Agarwal A K 2010 Measurement of number and size distribution of particles emitted from a mid-sized transportation multipoint port fuel injection gasoline engine *Fuel* **89**, Issue 9 pp2230-2233
- [23] Shankar R Udayakumar G and Sasikumar K 2008 Advanced Port Injection Solution for Motorcycle Application *SAE Technical Paper* **2008-28-0031**

Acknowledgment

The author acknowledges Prof. Safwat Wilson and Prof. Gaber Asar for being good advisers and for supporting technically and morally.